


Article

Hybrid Quantum Neural Network Image Anti-Noise Classification Model Combined with Error Mitigation

Naihua Ji ¹, Rongyi Bao ¹, Zhao Chen ¹, Yiming Yu ¹ and Hongyang Ma ^{2,*} 

¹ School of Information and Control Engineering, Qingdao University of Technology, Qingdao 266033, China; 13964863452@126.com (N.J.); 17854206520@163.com (R.B.); yim_7@icloud.com (Y.Y.)

² School of Science, Qingdao University of Technology, Qingdao 266033, China

* Correspondence: hongyang_ma@aliyun.com

Abstract: In this study, we present an innovative approach to quantum image classification, specifically designed to mitigate the impact of noise interference. Our proposed method integrates key technologies within a hybrid variational quantum neural network architecture, aiming to enhance image classification performance and bolster robustness in noisy environments. We utilize a convolutional autoencoder (CAE) for feature extraction from classical images, capturing essential characteristics. The image information undergoes transformation into a quantum state through amplitude coding, replacing the coding layer of a traditional quantum neural network (QNN). Within the quantum circuit, a variational quantum neural network optimizes model parameters using parameterized quantum gate operations and classical–quantum hybrid training methods. To enhance the system’s resilience to noise, we introduce a quantum autoencoder for error mitigation. Experiments conducted on FashionMNIST datasets demonstrate the efficacy of our classification model, achieving an accuracy of 92%, and it performs well in noisy environments. Comparative analysis with other quantum algorithms reveals superior performance under noise interference, substantiating the effectiveness of our method in addressing noise challenges in image classification tasks. The results highlight the potential advantages of our proposed quantum image classification model over existing alternatives, particularly in noisy environments.

Keywords: quantum neural network; variational quantum algorithm; image classification; error mitigation



Citation: Ji, N.; Bao, R.; Chen, Z.; Yu, Y.; Ma, H. Hybrid Quantum Neural Network Image Anti-Noise Classification Model Combined with Error Mitigation. *Appl. Sci.* **2024**, *14*, 1392. <https://doi.org/10.3390/app14041392>

Academic Editor: Yurii K. Gun’ko

Received: 2 January 2024

Revised: 4 February 2024

Accepted: 5 February 2024

Published: 8 February 2024



Copyright: © 2024 by the authors. Licensee MDPI, Basel, Switzerland. This article is an open access article distributed under the terms and conditions of the Creative Commons Attribution (CC BY) license (<https://creativecommons.org/licenses/by/4.0/>).

1. Introduction

In recent decades, machine learning has rapidly emerged as a foundational technology in the era of big data. Rooted in artificial intelligence and statistics, machine learning explores learning strategies and uncovers latent structures from the available data, enabling predictions and analyses through the derived models [1]. Its applications cover data mining and facial recognition, natural language processing, and identifying biomedical features, such as community detection on social networks [2], affecting all aspects of social life [2–4].

Quantum machine learning (QML) is an exceptionally promising interdisciplinary research direction, aiming to harness the capabilities of quantum computing alongside machine learning to overcome classical computing limitations. Numerous quantum algorithms have been proposed to enhance various machine learning tasks [5–7]. Image processing, a pivotal domain within digital image processing, encompasses all aspects of image acquisition, representation, processing, and analysis. With the widespread adoption of digital technology, image processing has found extensive applications, significantly impacting scientific research and playing a crucial role in fields such as medicine, engineering, and entertainment [8–11]. Image classification, a focal point in computer vision, has been a significant research target, employing techniques such as support vector machines and convolutional neural networks [12,13]. Chen et al. [14] innovatively incorporated classical

deep reinforcement learning algorithms, including experience replay and target networks, into variational quantum circuits with reduced weights. Additionally, a classification algorithm combining quantum computing with the decision tree algorithm [15,16] exists. The latter proposes the quantum representation of a binary classification tree with binary characteristics based on a probability method [16].

With the rapid advancement of quantum machine learning, a pivotal question arises: can quantum machine learning technology be trusted for image classification tasks amidst adversarial noise interference? Label noise, particularly in scenarios like medical image datasets with high-level label noise, can profoundly influence classification outcomes [17]. In autopilot systems, image classification identifies roads, pedestrians, vehicles, etc. Noise introduces inaccuracies in driving decisions, escalating the risk of traffic accidents. Video surveillance relies on image classification for object detection and identification. Noise may lead to false positives or negatives, diminishing the reliability of the monitoring system and compromising the accurate identification of potential threats [18,19]. Models are prone to overfitting noise labels, causing harm to representation learning and hindering generalization, thereby impacting diagnostic accuracy. Quantum error correction techniques demand substantial quantum bit resources, presenting implementation challenges [20–23]. To address this, error mitigation strategies, such as the autoencoders proposed by Zhang et al. [24], have proven effective for error correction without the need for additional quantum bits.

In a different domain, quantum neural networks (QNNs) represent a forefront research area that merges quantum computing with neural networks. Various implementations of quantum neural network models exist, with variational quantum circuits (VQCs) gaining significant attention [25–27]. In the era of noisy intermediate-scale quantum (NISQ), VQC offers practical feasibility as it can operate within the limitations of the currently available qubits. VQC design not only emphasizes the hardware implementation of quantum computing but also focuses on effective integration with classical computing to overcome the limitations of noise and errors in current quantum computing [28–31]. Recent research on quantum neural networks includes the work by Ban et al. [32], who proposed a quantum neural network (QNN) with multi-qubit interactions, transforming the quantum perceptron into a nonlinear classifier. The activation function chosen by the author is based on the adiabatic evolution of the system. Experimenting with other forms of activation functions is suggested to potentially enhance the network's performance. Higham et al. [33] proposed leveraging the quantum annealer to address classification tasks. However, overcoming the limitations of the binary nature of variables in quantum computing to handle more complex data types remains a challenge. In [34], a quantum recurrent neural network (QLSTM) is employed to optimize the training process of quantum reinforcement learning. Although the article mentions quantum error correction and noise resistance, practical applications still pose significant challenges in these aspects.

Building on the description provided earlier, this paper introduces a novel hybrid quantum network designed to tackle the performance challenges faced by quantum classifiers in the presence of noise interference. The hybrid network seamlessly combines a convolutional autoencoder (CAE) and a quantum neural network (QNN). Initially, the CAE is utilized to extract features from the image, and amplitude coding is introduced for encoding these features. The classification task is then executed using a variational quantum circuit (VQC). Furthermore, we integrate a quantum autoencoder to effectively reduce errors in quantum circuits, with the goal of enhancing the model's performance in the presence of noise interference while optimizing resource utilization.

This study investigates the dependability of quantum machine learning technology in image classification tasks under noise interference. It explores the integration of variational quantum circuits with error mitigation techniques to achieve robust image classification. The paper is organized as follows: Part II provides a comprehensive introduction to foundational theories and relevant work on convolutional autoencoders and quantum neural networks. Part III addresses noise-related issues in image classification, discusses the limi-

tations of traditional methods, and proposes a hybrid classical–quantum approach utilizing variational algorithms and error mitigation. Part IV outlines the experimental design and presents the results. The conclusion summarizes research findings and discusses prospects for future studies in the realm of quantum machine learning and image classification.

2. Background

2.1. Convolutional Automatic Encoder

The autoencoder (AE) represents a specialized instantiation within the broad domain of feedforward neural networks, featuring a distinctive architecture consisting of two essential components: an encoder and a decoder. The primary function of the encoder is to compress input data, facilitating a transformation into a low-dimensional code that encapsulates the latent space inherent in the input. Conversely, the decoder intricately reconstructs the output based on this condensed representation, orchestrating a process of data synthesis aimed at faithfully replicating the original input. This paradigm is typically characterized by the inclusion of fully connected layers in both the encoder and decoder modules.

In the evolutionary trajectory of neural network architectures, CAE emerges as a refined iteration, particularly distinguished by its enhanced efficacy in extracting textural features from images [35,36]. The CAE paradigm manifests a distinct structural augmentation, wherein the encoder is imbued with successive convolutional layers, and the decoder integrates transposed convolutional layers, all enveloping a strategically embedded sparse inner layer. The consequential outcome is an autonomously functioning CAE encoder that assumes a pivotal role in the extraction of low-dimensional representations, specifically tailored for the realms of image feature extraction and the reduction in dimensionality. The training regimen for the CAE involves exposure to raw, unprocessed image data, facilitating the acquisition of a profound understanding of a low-dimensional representation. Unlike the traditional AE, CAE deviates by utilizing convolutional layers in both the encoder and decoder networks, replacing the previous reliance on fully connected layers.

The structural augmentation of the CAE is not arbitrary but rooted in its pursuit of heightened performance in processing image data while meticulously preserving spatial structural information. A defining attribute of the convolutional layers in the CAE is their demonstration of translation invariance, a quality that imparts a remarkable capability to capture local features and spatial relationships within the intricate tapestry of image data. This intrinsic characteristic contributes substantively to the CAE's efficacy, rendering it a potent tool in the realm of image processing and analysis. In summary, the CAE represents a sophisticated and refined instantiation of neural network architectures, with its convolutional underpinnings endowing it with a distinctive prowess in the extraction and preservation of intricate features within the visual domain. In this paper, we only utilize the encoder for image feature extraction and dimensionality reduction.

2.2. Quantum Neural Network

Quantum circuit-based networks, as demonstrated by Matsui and Maeda's method [37,38], utilize quantum gate circuits featuring rotation and controlled-NOT gates. These circuits process quantum states as inputs, and a weight update process, akin to traditional forward propagation algorithms, is presented in complex number representation. Matsui and Maeda introduced an innovative approach to constructing neural networks based on quantum gate circuits. Their methodology employs fundamental quantum computing components, specifically a single-qubit quantum rotation gate and a controlled-NOT gate. These gates collectively form the neural network, with quantum states serving as input. The network's weight update process adheres to a complex-valued formulation derived from the traditional forward propagation algorithm. The network architecture, visually depicted in accompanying diagrams, showcases the integration of quantum gates in the neural network framework.

Variational quantum circuits, pivotal in quantum machine learning, comprise three essential components. First, the feature map F facilitates the mapping of classical data points x onto a z -qubit quantum state $|\varphi(x)\rangle$. This state preparation is expressed as

$$|\varphi(x)\rangle = F(x)|0\rangle^{\otimes z} \tag{1}$$

Later, an ansatz, denoted by α and parameterized by a vector θ , operates on the quantum state through a sequence of entangling and rotation gates. The resulting quantum state is then determined as

$$|\varphi(x, \theta)\rangle = \alpha(\theta)|\varphi(x)\rangle \tag{2}$$

Finally, the observable O is measured, recording eigenvalues corresponding to the resultant quantum state. The QNN diagram is shown in Figure 1.

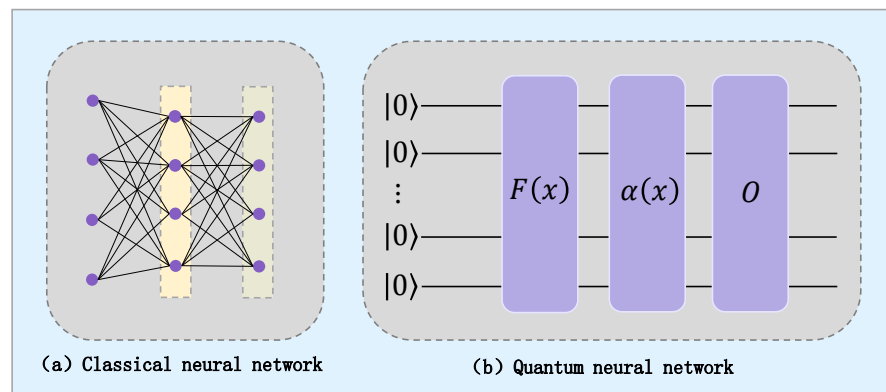


Figure 1. (a) Classical neural networks typically comprise three layers: an input layer, a hidden layer, and an output layer. Each layer contains multiple neurons, and the connections between neurons have varied weights. (b) In contrast, QNN involves three layers: $F(x)$ serves as the coding layer, $\alpha(x)$ acts as the variable layer, and O functions as the measurement layer.

In the realm of machine learning, the variational quantum circuit is executed multiple times with specific inputs x and parameter vectors θ . This iterative process allows the circuit’s expectation value, denoted by f , to approximate the desired output:

$$f(x, \theta) = \langle \varphi(x, \theta) | O | \varphi(x, \theta) \rangle \tag{3}$$

This expectation value serves as a crucial approximation for the model’s output in various machine learning applications, where the variational quantum circuit offers a quantum-enhanced approach to computational tasks.

3. Construction of Mixed Variational Quantum Neural Network and Error Mitigation Model

Initially, a classical convolutional autoencoder is used for image feature extraction. Following this, amplitude coding is applied to encode the extracted feature vectors, and the resulting quantum states are input into the quantum classifier for classification tasks. The classifier consists of a quantum neural network and a quantum self-encoder. The variational quantum circuit predicts the input quantum state, followed by error mitigation through the quantum self-encoder. The classification process is then finalized through measurement.

3.1. CAE (Feature Extraction and Dimension Reduction)

The convolutional autoencoder (CAE), inspired by Masci’s seminal work [39], serves as a paradigm in unsupervised learning neural network models, designed to proficiently capture data representations and extract salient features.

CAE Architecture and Weight Sharing: In preserving spatial locality, CAE employs weight sharing across all positions in the input, adhering to a structural resemblance with

traditional autoencoders. The latent representation, denoted as h^m , for the m -th feature map of a single-channel input tensor, is intricately expressed as

$$h^m = \omega(t * W^m + b^m) \tag{4}$$

where ω represents the activation function, and $*$ symbolizes 2D convolution. Reconstruction Process in CAE: The reconstruction process within CAE unfolds through a linear combination of fundamental image blocks contingent upon the latent code. The reconstruction equation takes the form

$$I = \omega\left(\sum_{m \in H} h^m * \tilde{W}^m + c\right) \tag{5}$$

where H denotes the set of latent feature maps, \tilde{W} embodies a two-dimensional weight-flipping operation, and $*$ denotes the 2D convolution operation. Cost Function and Optimization in CAE: The imperative cost function guiding CAE's training regimen is the mean square error (MSE), formalized as

$$E(\theta) = \frac{1}{2n} \sum_{i=1}^n (t_i - I_i)^2 \tag{6}$$

To minimize this cost function, the optimization process leverages backpropagation to compute gradients of the error function concerning the parameters. The gradients are ascertained through convolution operations, expressed as

$$\frac{\partial E(\theta)}{\partial W^m} = t * \delta h^m + \tilde{h}^m * \delta I \tag{7}$$

where δh and δI denote the incremental changes in hidden states and reconstruction, respectively.

Stochastic gradient descent plays a crucial role in optimizing the CAE model by iteratively adjusting weights to improve overall performance. Grayscale images, with their straightforward structure, allow for direct feature extraction. However, for color images, conversion of RGB values to corresponding grayscale values is necessary before applying this algorithm. Figure 2 illustrates an example of multi-channel image feature extraction.

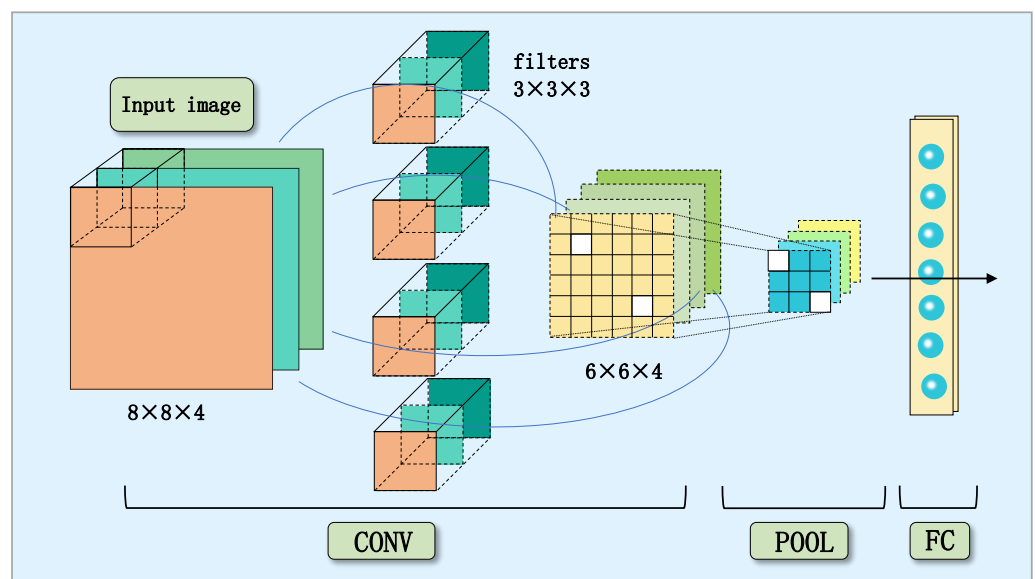


Figure 2. The image includes convolution automatic encoder for feature extraction and dimensionality reduction, and convolution automatic encoder includes convolution layer (CONV), pooling layer (POOL), and full-connection layer (FC).

3.2. Amplitude Coding

In this study, we explore the utilization of amplitude encoding as an alternative to the encoding layer within QNN for image feature representation. The primary objective is to alleviate the complexity associated with traditional classification models. Moreover, employing amplitude coding in advance holds the potential to mitigate noise interference and bolster the robustness of resulting quantum states. This proactive approach contributes to the improvement of accuracy and stability in image classification tasks.

Amplitude encoding serves as a powerful technique for mapping classical data onto quantum states [40]. Through this process, classical image data undergo a transformation, becoming embedded within the unique characteristics of quantum states. The intrinsic ability of quantum states to handle complex coherence and entanglement positions amplitude encoding as a potentially superior method for certain image processing tasks, particularly those requiring intricate feature extraction and classification.

A notable advantage of early amplitude encoding lies in its capability to mitigate noise interference. The resulting quantum states exhibit enhanced robustness, a critical factor in the context of image classification. The reduction in noise interference contributes to an overall improvement in accuracy and stability, making amplitude encoding a valuable preprocessing step. For a given dataset, $D' = \{t^j\}_{j=1}^{l'}$, $t^j = (t_1^j, t_2^j, \dots, t_n^j)$, l' represents the total number of samples in the dataset, and n represents the number of features per sample. the representation function is defined as

$$f(D') = \frac{1}{C} \sum_{j=1}^{l'} \sum_{i=1}^n t_i^j |i, j\rangle \quad (8)$$

where C is the normalization constant. This representation provides a structured basis for further exploration and analysis. Efficiency in amplitude encoding is highlighted by the fact that, for datasets with a length ln that is a power of 2, only $\log(ln)$ quantum bits are required to encode ln amplitudes. The amplitude coding problem can be simplified to give a single-point set $T = \{t = (t_0, \dots, t_{N-1})\} \subset \mathcal{R}^N$. Neglecting the normalization constant

$$f(T) = \sum t_i |i\rangle \quad (9)$$

To optimize runtime considerations, the introduction of N quantum bits allows for an expanded choice of amplitude encoding bases. The selection of the W -state basis exemplifies the strategic choices made in our approach.

Here, we use bottom-top amplitude coding. The adoption of bottom-top amplitude encoding involves the construction of a quantum circuit with $O(n)$ width and $O(\lceil \log_2 N \rceil)$ depth. Notably, the structure of the angle tree, specifically the leftmost subtree $(\alpha_0, \alpha_1, \alpha_3)$, corresponds to the output qubit, with others serving as auxiliary qubits. The construction is meticulously illustrated in accompanying diagrams. The build form is shown in the following Figure 3.

In conclusion, our investigation into amplitude encoding as a preprocessing step for image feature representation within a quantum framework highlights its potential to enhance classification models. The decrease in complexity, reduction in noise interference, and the enhanced robustness of quantum states collectively contribute to a more accurate and stable image classification process. The strategic considerations in amplitude encoding efficiency and the structured circuit construction further underscore the viability of this approach in the realm of quantum image processing.

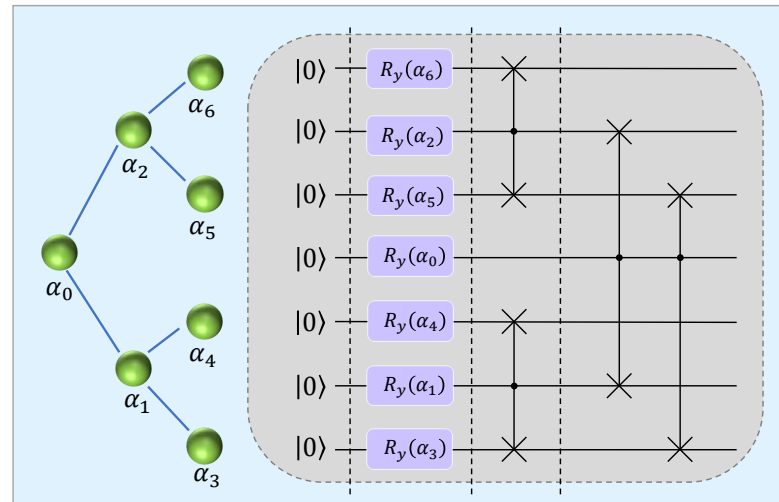


Figure 3. The figure shows an example of bottom-top amplitude coding. The black dots in the circuit represent the control relationship between qubits, and the crosses represent the interaction or coupling between two or more qubits. Where the quantum logic gate corresponding to the circuit in the figure is the controlled SWAP gate, which is used to exchange auxiliary bits and output bit quantum states.

3.3. Construction of QNN by Variational Quantum Circuit

In this research endeavor, we delve into the realm of quantum machine learning, specifically exploring the integration of amplitude encoding within QNN for image classification. Our methodology draws inspiration from the QNN model proposed by Wu et al. [41], where VQC is leveraged for constructing the QNN. This novel approach seeks to harness the quantum advantage in processing and representing image features through the amplitude encoding scheme.

Quantum neural networks operate on quantum input data through a sequence of parameter-dependent quantum gates. The representation of a QNN can be expressed as:

$$U(\theta) = \prod_{c=1}^N V_c U_c(\theta_c) \tag{10}$$

Here, θ represents the trainable parameters, V_c and $U_c(\theta_c)$ are quantum gates acting on the data, forming a powerful quantum circuit capable of complex transformations. Given an input, x , and trainable parameters θ , the amplitude encoding scheme transforms the input into a quantum state

$$|\Psi\rangle = U_\theta|x\rangle \tag{11}$$

For binary classification, observable projections O_k^+ and O_k^- on the PauliZ basis are defined, corresponding to spin +1 and -1, respectively.

$$P_1(|\Psi\rangle) = \langle\Psi|O_k^+|\Psi\rangle \tag{12}$$

Similarly, $P_2(|\Psi_i\rangle)$ is defined for Class 2. Classification for a new input $|\Psi_i\rangle$ is determined based on the product of probabilities, with the class receiving the highest probability being assigned as the prediction. The output of the QNN is based on the measurement results of quantum bits. The expectation value E is used as the QNN output, defined as:

$$E = \langle\Psi_x|U^\dagger(\theta)VU(\theta)|\Psi_x\rangle \tag{13}$$

Here, V is a linear combination of Pauli operators applied to the observable of the reading quantum bit, providing a probabilistic representation of the quantum state.

The construction of the quantum classifier involves a variational quantum circuit utilizing s data quantum bits. These bits load local features extracted through CAE and

amplitude encoding. The prediction is obtained through a single quantum bit output, with the number of reading quantum bits determined by the classification task. In our approach, the Ising coupling gate entangles the qubits. Similar to classical neural networks, the variable component subgate functions as a neuron, and the block serves as a layer in QNN. A block is defined as m gates continuously acting on m pairs of data and readout qubits. This block can be repeated to construct a complex QNN with more parameters. The prediction layer for the data is denoted as $U_p(\theta_p)$, and the predicted result for a given instance x is represented as:

$$y' = \langle \Psi_T | U_p^\dagger(\theta_p) V U_p(\theta_p) | \Psi_T \rangle \tag{14}$$

where $|\Psi_T\rangle$ is the quantum state T whose extracted features are encoded by amplitude. The circuit is shown in Figure 4. The prediction layer utilizes a VQC that employs double-qubit parametrized gates, inducing entanglement between quantum bits. The optimization strategy follows the scheme proposed by Ren et al. [42], incorporating the cross-entropy as the chosen loss function. The loss function is defined as the negative log-likelihood of the predicted probabilities compared to the true labels. For a binary classification task, it takes the form:

$$\mathcal{L}(f(x; \theta), A) = - \sum_k r_k \log j_k \tag{15}$$

Here, $A \equiv (r_1, \dots, r_m)$ represents the labels in one-hot encoding, f is the hypothesis function determined by the QNN, and $G \equiv (j_1, \dots, j_m)$ represents the probability of output categories. Gradient descent is then employed to iteratively adjust the parameters to minimize the loss function.

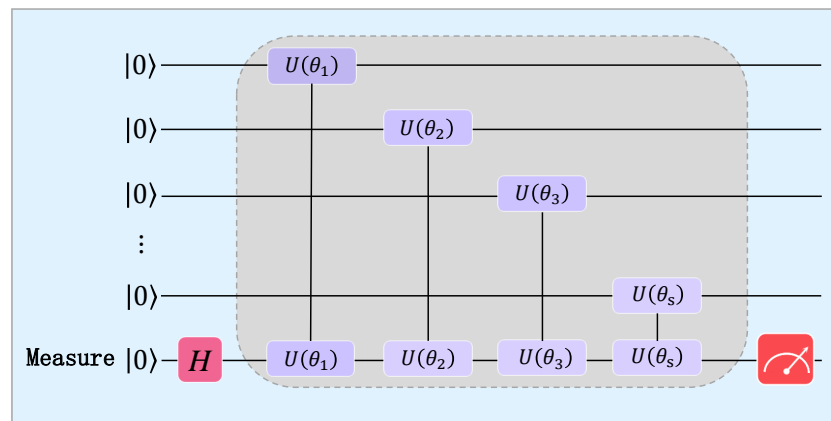


Figure 4. The circuit of the predictor uses s data qubits to load the local features extracted using the coding unit, and uses a readout qubit to output the prediction result.

More specifically, for the amplitude coding scheme:

$$j_k = \langle x | U_\theta^\dagger O_k U_\theta | x \rangle \tag{16}$$

The derivative of the loss concerning the parameters is computed through the parameter shift rule. For a binary classification task, it takes the form:

$$\frac{\partial \mathcal{L}(f(x; \theta), A)}{\partial \theta} = - \sum_k \frac{r_k}{j_k} \frac{\partial j_k}{\partial \theta} \tag{17}$$

The optimization strategy involves iteratively updating the parameters using gradient-based optimization techniques, ensuring convergence to a set of parameters that minimizes the loss function.

In conclusion, our research navigates the intricate landscape of quantum machine learning, integrating amplitude encoding within the QNN framework. The combination of

amplitude encoding, VQC, and optimization strategies contributes to the development of robust quantum classifiers with potential applications in image classification tasks.

3.4. Error Mitigation

Our discussion utilizes the concepts outlined in [24]. In this work, the authors employ a generic detection-based error-mitigation strategy utilizing quantum autoencoders, presenting a novel protocol for quantum error correction. The method crucially relies on the identification of singular unitary operators capable of compressing quantum data from the entirety of the Hilbert space to a designated subspace, which is particularly effective when specific quantum datasets exhibit discernible underlying structures. The assumption is made that the Hilbert space and the supporting subspace \mathcal{S} share common underlying structures. For clarity, parameters $X \equiv \dim \mathcal{H}$ and $M \equiv \dim \mathcal{S}$ are defined. The subspace \mathcal{S} is presumed to have an orthogonal basis $|S_i\rangle$, with the introduction of a latent subspace \mathcal{L} characterized by $\dim \mathcal{L} = M$, defined by another orthogonal basis $|L_i\rangle$. The encoding unitary operator U_e is introduced with flexibility, allowing it to be set as any unitary satisfying $\langle L_i|U_e|S_i\rangle = 1$. These elements collectively form a comprehensive framework for a quantum error-correction protocol utilizing autoencoders and singular unitary operators, offering insights into the challenges and strategies for effective error mitigation in quantum information processing systems.

Using the unitary encoding U_e to manipulate the encoded and variational processed quantum state \tilde{q} , we denote the tilde as representing a noisy quantum state and the prime as indicating reduced errors. The compressed noisy quantum state $\tilde{q}_c \equiv U_e \tilde{q} U_e^\dagger$ transforms into $(1 - \epsilon)q_c + \epsilon U_e q^{error} U_e^\dagger$, where $\{M_L\}$ and $\{M_J\}$ are projectors onto \mathcal{L} and orthogonal projectors, respectively. Considering the subspace of q_c , we have

$$M_L \tilde{q}_c M_L^\dagger = (1 - \epsilon)q_c + \epsilon U_e \Lambda_s^{error} U_e^\dagger \tag{18}$$

where $\Lambda_s^{error} \equiv M_S q^{error} M_S^\dagger$, Λ_s^{error} to the supporting subspace \mathcal{S} . When ϵ is small, the states gather in the potential subspace \mathcal{L} , and they become

$$q'_c = \frac{(1 - \epsilon)q_c + \epsilon U_e \Lambda_s^{error} U_e^\dagger}{1 - \epsilon + \epsilon \text{tr}(\Lambda_s^{error})} = [p_s + O(\epsilon^2)] + [\epsilon + O(\epsilon^2)] U_e \Lambda_s^{error} U_e^\dagger \tag{19}$$

Here, ϵ and $\text{tr}(\Lambda_s^{error})$ determine higher-order terms. These states are projected into the garbage subspace with a low probability of $1 - p_s$. In such cases, errors are identified, and the corresponding quantum data are eliminated. Finally, the error-mitigated state is obtained by applying the decoding unitary U_e^\dagger to q'_c , where $q' \equiv U_e^\dagger q'_c U_e$.

We use programmable circuits, as shown in the figure. Global entanglement unitary $e^{-iH\tau}$ and a set of arbitrary single-qubit rotations exist in each layer (we set $\tau = 1$), where

$$H = \sum_{i=1}^n \sum_{\sigma=x,z} h_i^\sigma q_{ci}^\sigma + \sum_{i=1}^n \sum_{j \geq i} \sum_{\sigma=x,y,z} J_{i,j}^\sigma q_{ci}^\sigma q_{cj}^\sigma \tag{20}$$

Here, h_i^σ and $J_{i,j}^\sigma$ are adjustable parameters necessitating iterative experimentation to identify the suitable dimension of the subspace $\dim \mathcal{L}$ for compression. Notably, a shallow error-mitigation circuit with $N_{ly} = 1$ suffices, and increasing N_{ly} provides no additional benefit. Consequently, our approach involves training a single-layer shallow error-mitigation circuit to compress input states to the subspace. During compression, the last qubit is considered an "auxiliary qubit," as it is not utilized for classification. Thus, no additional qubits are required, enabling error mitigation within the constraints of the currently available limited qubits. The compressed quantum states are effectively confined to the hidden subspace, while errors are retained outside it, subsequently eliminated through measurement and post-selection. The working principle of the error mitigation layer is shown in Figure 5.

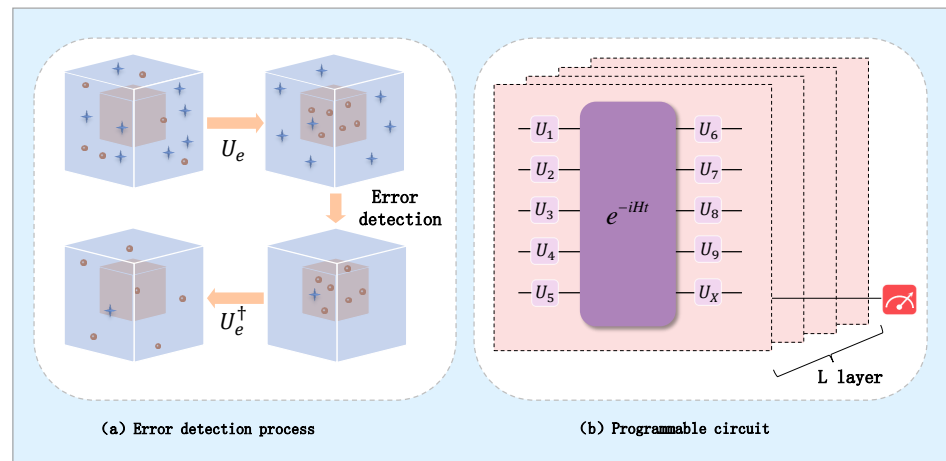


Figure 5. (a) The process of error mitigation. U_e moves error-free items to the potential subspace, while most errors remain in the garbage subspace. Then, we use measurements to project the state onto the potential subspace and remove errors in the garbage subspace. Finally, U_e is used to recover quantum data. The dots represent standard qubits and the stars represent incorrect qubits. (b) The programmable circuit of quantum self-encoder U_e with L-layer network.

4. Simulation and Analysis

4.1. Experimental Settings

In this study, we chose classical MNIST [43] and FashionMNIST [44] datasets for image classification tasks, both widely used benchmark datasets. MNIST consists of handwritten digit images, and we conducted benchmark testing using the MNIST dataset in Section 4.2.1. FashionMNIST includes images of clothing and accessories, and we performed noise-resistant experiments using the FashionMNIST dataset in Section 4.2.2. Our objective is to explore quantum computing-based image classification in the noisy intermediate-scale quantum (NISQ) era. Considering the potential impact of noise on quantum devices in practical applications during the NISQ era, we specifically focused on the influence of noise on image classification tasks. In our simulation experiments, we employed the depolarizing channel model to simulate the effects of noise, a widely used noise model for describing real quantum devices.

We utilized the PennyLane library, which offers robust support for quantum neural networks and seamlessly integrated it with the PyTorch interface to facilitate the training process of quantum and classical neural networks [45]. To simulate the effects of quantum computing, we selected the Qulacs quantum simulator [46], known for efficiently simulating the evolution of quantum circuits. In our experimental setup, we set the learning rate to 0.001, a common hyperparameter setting to balance model convergence speed and stability. Additionally, we defined the batch size to optimize training efficiency and framed the task as a four-class classification task to align more closely with real-world applications. In our experiment, after testing, we set up 8 data qubits, four classifications require 2 readout qubits, and the entire circuit has 56 adjustable parameters. In this simulation experiment, we aim to enhance our understanding of how noise affects image classification tasks in quantum computing. Furthermore, we aim to assess the performance of the suggested hybrid classical QNN classification model in the NISQ era. Additionally, we aim to demonstrate the effectiveness of our combined training strategy for hybrid quantum neural networks and error-mitigation strategies in image classification, as well as the model's robustness and generalization capabilities in the presence of noise.

4.2. Simulation and Analysis

In this section, we conduct several sets of experiments to identify the optimal model and optimization strategy through training and testing. The ultimate results are presented. The accuracy of the model proposed in this article for image classification is comparable to

that of current quantum classifiers. Moreover, in simulated noisy environments, it consistently maintains high accuracy, demonstrating superior anti-noise capabilities compared to other models.

4.2.1. MNIST Accuracy Test

In this experimental section, we employed the classification model designed in this paper to perform a four-class classification task on the MNIST dataset. Each sample in the MNIST dataset is a grayscale image of size 28×28 pixels. The dataset used here is MNIST, which is a collection of digit images covering the numbers 0 to 9. In this experiment, we have selected a subset of images containing digits 0 to 3 for conducting a four-class classification. We selected 400 training image samples (100 samples for each of the digits 0, 1, 2, and 3) and 200 test image samples. For the four-class classification task, four measurements and outputs were set at the end of the circuit. The variational quantum circuit was tested with four, five, and six layers. In the benchmark test, optimization was conducted over 100 epochs. As shown in Figure 6, the classification capability does not necessarily improve with an increase in variational blocks in our limited design. The best classification performance was achieved with five layers of variational quantum blocks, reaching a maximum accuracy of 0.98. Therefore, in the subsequent experiments, we consistently adopted five layers of variational quantum blocks, measuring the first four quantum bits for the four-class classification.

The classification model designed in this paper achieved a classification accuracy of over 0.9 in a relatively short number of epochs. The accuracy obtained in the four-class classification study using the MNIST dataset is not significantly superior to the current best classical classification algorithms. However, the demonstrated classification accuracy and optimization of the model affirm the feasibility of our designed classifier in image classification, showcasing commendable classification performance.

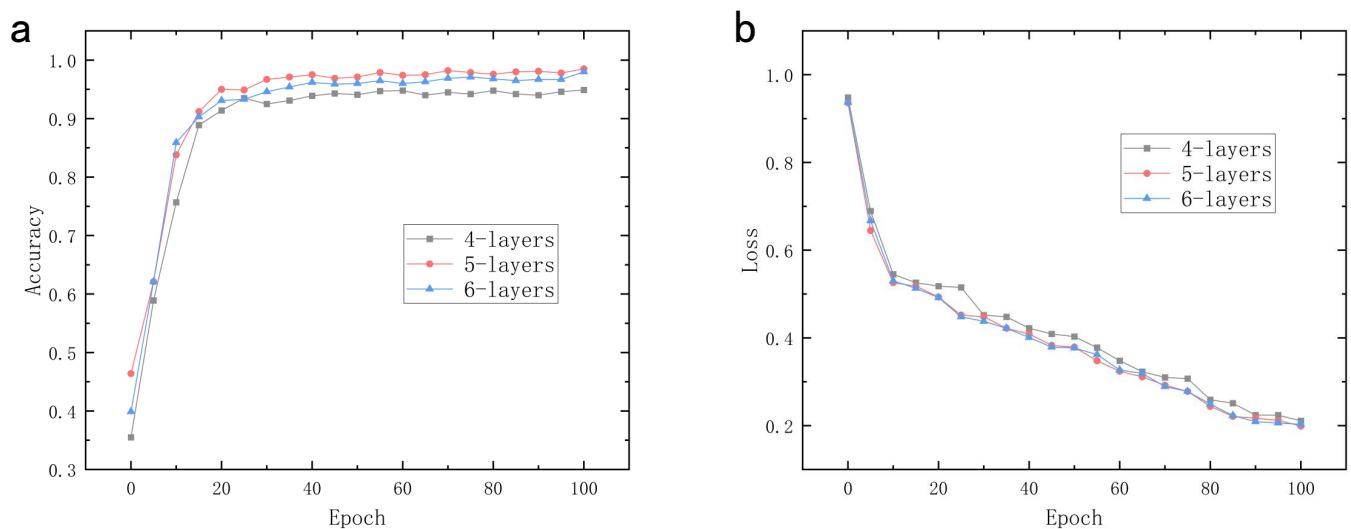


Figure 6. (a) Test accuracy of classification models using variable component sub-blocks of different layers on MNIST datasets. (b) Test loss of classification models using variable component sub-blocks of different layers on MNIST datasets.

4.2.2. FashionMNIST Accuracy and Anti-Noise Test

In this experimental section, we conducted simulation experiments on the Fashion-MNIST dataset to explore the performance and noise resilience of our designed hybrid QNN denoising classification model in image classification tasks. FashionMNIST, a commonly used benchmark dataset for image classification, contains images of clothing and accessories. We selected images from four categories in FashionMNIST, with each category having 150 training samples, totaling 600 image samples, and 400 test samples. In the

experiments, we consistently utilized five variational quantum blocks as the building units for the classifier. These variational quantum blocks manipulate the input quantum states through a series of quantum gates and parameterized operations. To simulate noise effects in real-world scenarios, we set two different levels of noise: 0.03 and 0.1. These noise values represent mild and significant random perturbations on pixel values in the images. The experimental results will be evaluated using metrics such as accuracy and loss values to gain insights into the performance and noise resilience of variational quantum blocks in image classification tasks on the FashionMNIST dataset.

As depicted in the experimental results, the curves in Figure 7 illustrate the generalization ability of our model in image classification tasks. Even under the slight interference of noise with a value of 0.03, our model still achieves an accuracy of around 0.92. Under the more substantial interference of noise with a value of 0.1, the accuracy remains above 0.85, approaching 0.9, demonstrating commendable performance. Table 1 shows the confusion matrix of the classification results of the 100th cycle without noise interference. These results indicate the effectiveness of our design and suggest further potential enhancements. Enhancing system robustness involves incorporating more intricate quantum transformation layers in the experimental framework, and employing optimization methods can elevate the system’s classification performance. Error mitigation plays a significant role in mitigating noise effects on the images to a certain extent.

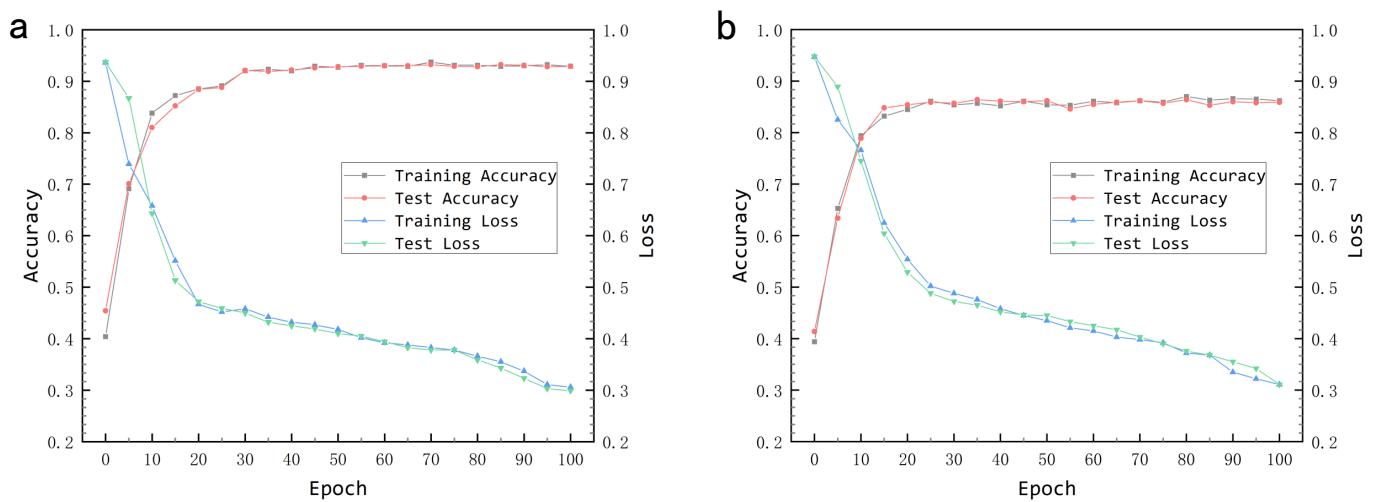


Figure 7. (a) The training and testing accuracy and loss of the classification model using five-layer variable component sub-blocks on FashionMNIST datasets are carried out in the depolarization channel with a noise value of 0.03. (b) The training and testing accuracy and loss of the classification model using five-layer variable component sub-blocks on FashionMNIST datasets are carried out in the depolarization channel with a noise value of 0.1.

Table 1. Confusion matrix of classification results on FashionMNIST.

	True Class1	True Class2	True Class3	True Class4
Prediction class1	95	3	5	0
Prediction class2	1	91	2	4
Prediction class3	2	3	90	1
Prediction class4	2	3	3	95

We compare the model proposed in this paper with other recent quantum neural network classification algorithms in noisy environments. Here, we classify the test subset of the FashionMNIST dataset using SQNN [47] and RQNN [48]. This experiment still selected 400 test samples. The range of noise is set from 0.01 to 0.1. Figure 8 illustrates that the accuracy of our newly proposed classifier improves as the noise level increases,

and its accuracy under noise interference surpasses that of SQNN and RQNN. Our method effectively mitigates the impact of line noise on experimental results.

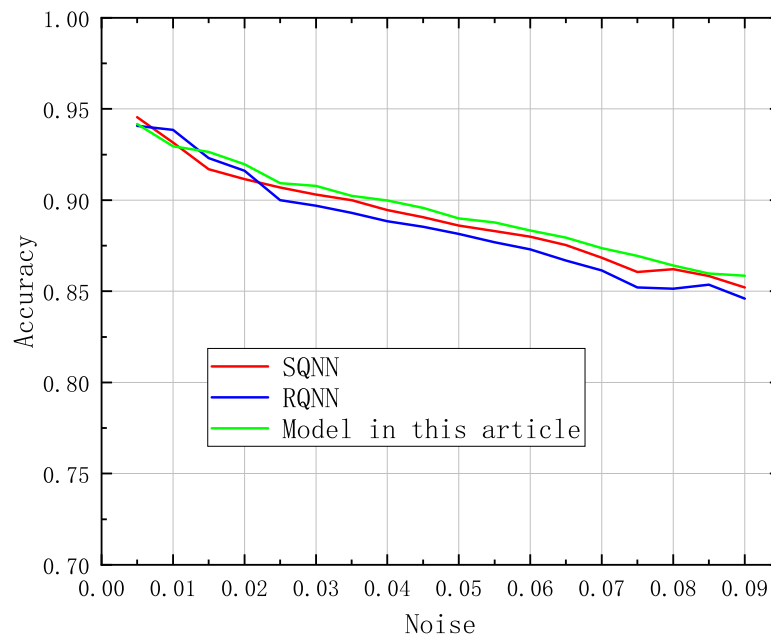


Figure 8. RQNN, SQNN, and the model presented in this article analyze and compare the quaternary classification of the FashionMNIST dataset.

4.2.3. Comparison of Noise Effects

In this section, we compare the hybrid variational QNN model proposed in this paper with other quantum algorithms, specifically classical QNN image classification and QCNN image classification [49]. The circuit diagrams for the methods used by QNN and QCNN are depicted in Figure 9. For QNN, parameterized rotation gates and entanglement gates are applied. Given a specific number of layers, these gates transform the qubit states. The transformed qubit states are then measured by obtaining the expectation value of the Hamiltonian. These measurements are decoded into the appropriate output data format. Subsequently, the parameters are updated via the optimizer. QCNN convolutional circuits identify hidden states by applying multiple qubit gates between adjacent qubits. The quantum convolutional layer applies a filter to the input feature map, generating a new feature map composed of updated data. In cases where the system size is small, fully connected circuits are employed to predict classification results.

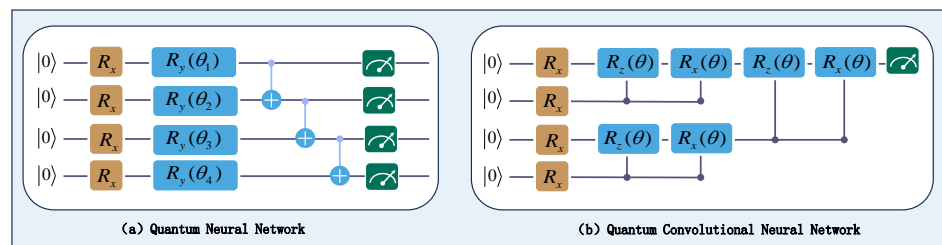


Figure 9. (a) QNN diagram illustrating input, parameters, and linear entanglement structure. (b) Example of quantum convolutional layer for image classification.

Comprehensive model performance and training efficiency: Our model utilizes eight data qubits and incorporates five layers of variational blocks. In this classification task, the number of variables and optimization efficiency of our model are comparable to those of QNN and QCNN. Our model can achieve higher classification accuracy faster, but after

more training iterations, the classification accuracy of the three methods is close in a noise-free environment. We conduct quaternary classification tests for MNIST and FashionMNIST datasets in environments with noise values of 0, 0.03, and 0.1, respectively. The variable component sub-block is set to 5, and the test results are shown in Figure 10. As seen in the figure, in FashionMNIST image classification, the accuracy of our classification model can reach about 0.97 in a noise-free environment, which is comparable to other quantum classification algorithms. In the noise test with 0.03 slight noise, our model exhibits clear advantages and can still achieve a classification accuracy of more than 0.9. When the noise reaches 0.1, our model can still achieve an accuracy of more than 0.85, which is approximately 20% higher than that of the QNN model and about 17% higher than that of the QCNN model.

Here, we demonstrate that our proposed hybrid variational QNN framework can achieve high accuracy in multivariate image classification. Our quantum neural network, combined with error mitigation, effectively reduces the impact of noise on experimental results. Experiments conducted on FashionMNIST datasets reveal that the classification performance of our model surpasses that of existing quantum classifiers.

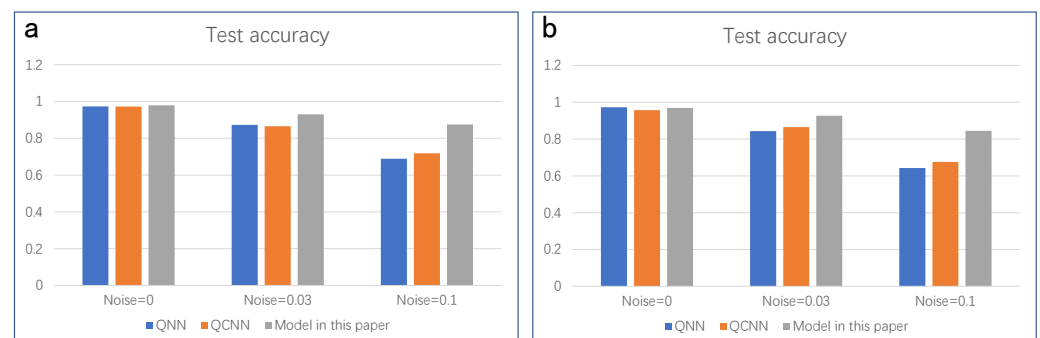


Figure 10. (a) The classification performance of the three classification methods of QNN, QCNN, and this model in the environment of different noise values of MNIST datasets. (b) Comparison with FashionMNIST.

5. Conclusions

In this study, we successfully developed a hybrid variational quantum neural network architecture to tackle the challenge of noise interference in quantum image classification. Our architecture utilizes a convolutional autoencoder for feature extraction, offering robust support for subsequent variational quantum circuits by capturing essential image features. The use of amplitude coding simplifies the model by directly converting image information into a quantum state, reducing complexity and enhancing the model's resistance to noise. To further improve the system's anti-noise capabilities, we introduce a quantum autoencoder for error mitigation. Experimental results demonstrate a substantial improvement in image classification accuracy in noisy environments, achieving a high level of 92%. Compared to other traditional quantum algorithms, our method exhibits superior robustness, confirming the excellent performance of our hybrid quantum neural network classifier in addressing noise interference in image classification tasks.

This study introduces a novel approach to advancing quantum image classification, showcasing significant potential with the mixed variational quantum neural network architecture, especially in noisy environments. The experimental demonstration, using quaternary classification, serves as an illustrative example of our algorithm's performance. Future research directions may involve exploring the method's efficacy in more complex datasets and practical applications, along with gaining a deeper understanding of the integration between quantum computing and machine learning. While there may still be some disparity between our model and its classical counterpart, ongoing efforts will concentrate on refining our model to minimize resource consumption and ensure its practical utility in future quantum computers. We are optimistic that our model will play a

pivotal role in supporting the widespread application of quantum computing in the field of image processing.

Author Contributions: Writing—original draft, N.J. and R.B.; data curation, N.J. and R.B.; formal analysis, Z.C. and Y.Y.; methodology, R.B. and H.M. All authors have read and agreed to the published version of the manuscript.

Funding: This work was supported by the Natural Science Foundation of Shandong Province, China (Grant Nos. ZR2021MF049), and Joint Fund of Natural Science Foundation of Shandong Province (Grant Nos. ZR2022LLZ012).

Institutional Review Board Statement: Not applicable.

Informed Consent Statement: Not applicable.

Data Availability Statement: The data are contained within the article.

Conflicts of Interest: The authors declare no conflicts of interest.

References

- Alzubi, J.; Nayyar, A.; Kumar, A. Machine learning from theory to algorithms: An overview. *J. Phys. Conf. Ser.* **2018**, *1142*, 012012. [[CrossRef](#)]
- Khanday, A.M.U.D.; Wani, M.A.; Rabani, S.T.; Khan, Q.R. Hybrid Approach for Detecting Propagandistic Community and Core Node on Social Networks. *Sustainability* **2023**, *15*, 1249. [[CrossRef](#)]
- Yaman, M.A.; Subasi, A.; Rattay, F. Comparison of random subspace and voting ensemble machine learning methods for face recognition. *Symmetry* **2018**, *10*, 651. [[CrossRef](#)]
- Jin, B.; Cruz, L.; Gonçalves, N. Deep facial diagnosis: Deep transfer learning from face recognition to facial diagnosis. *IEEE Access* **2020**, *8*, 123649–123661. [[CrossRef](#)]
- Alchieri, L.; Badalotti, D.; Bonardi, P.; Bianco, S. An introduction to quantum machine learning: From quantum logic to quantum deep learning. *Quantum Mach. Intell.* **2020**, *3*, 1–30. [[CrossRef](#)]
- Skolik, A.; Jerbi, S.; Dunjko, V. Quantum agents in the gym: A variational quantum algorithm for deep q-learning. *Quantum* **2022**, *6*, 720. [[CrossRef](#)]
- Caro, M.C.; Huang, H.Y.; Cerezo, M.; Sharma, K.; Sornborger, A.; Cincio, L.; Coles, P.J. Generalization in quantum machine learning from few training data. *Nat. Commun.* **2022**, *13*, 4919. [[CrossRef](#)]
- Yu, Y.; Gao, J.; Mu, X.; Wang, S. Adaptive LSB quantum image watermarking algorithm based on Haar wavelet transforms. *Quantum Inf. Process.* **2023**, *22*, 180. [[CrossRef](#)]
- Mu, X.; Wang, H.; Bao, R.; Wang, S.; Ma, H. An improved quantum watermarking using quantum Haar wavelet transform and Qsobel edge detection. *Quantum Inf. Process.* **2023**, *22*, 223. [[CrossRef](#)]
- Egmont-Petersen, M.; de Ridder, D.; Handels, H. Image processing with neural networks—A review. *Phys. Rev. Lett.* **2002**, *35*, 2279–2301.
- Fadnavis, S. Image interpolation techniques in digital image processing: An overview. *Int. J. Eng. Res. Appl.* **2014**, *4*, 70–73.
- Chandra, M.A.; Bedi, S.S. Survey on SVM and their application in image classification. *Int. J. Inf. Technol.* **2021**, *13*, 1–11. [[CrossRef](#)]
- Sun, Y.; Xue, B.; Zhang, M.; Yen, G.G.; Lv, J. Automatically designing CNN architectures using the genetic algorithm for image classification. *IEEE Trans. Cybern.* **2019**, *50*, 3840–3854. [[CrossRef](#)]
- Chen, S.Y.C.; Yang, C.H.H.; Qi, J.; Chen, P.Y.; Ma, X.; Goan, H.S. Variational quantum circuits for deep reinforcement learning. *IEEE Access* **2020**, *8*, 141007–141024. [[CrossRef](#)]
- Lu, S.; Braunstein, S.L. Quantum decision tree classifier. *Quantum Inf. Process.* **2014**, *13*, 757–770. [[CrossRef](#)]
- Heese, R.; Bickert, P.; Niederle, A.E. epresentation of binary classification trees with binary features by quantum circuits. *Quantum* **2022**, *6*, 676. [[CrossRef](#)]
- Khanal, B.; Bhattarai, B.; Khanal, B.; Linte, C.A. Improving Medical Image Classification in Noisy Labels Using only Self-supervised Pretraining. In *MICCAI Workshop on Data Engineering in Medical Imaging*; Springer Nature: Cham, Switzerland, 2023; pp. 78–90.
- Tian, C.; Fei, L.; Zheng, W.; Xu, Y.; Zuo, W.; Lin, C.W. Deep learning on image denoising: An overview. *Neural Netw.* **2020**, *131*, 251–275. [[CrossRef](#)]
- Rasti, B.; Scheunders, P.; Ghamisi, P.; Licciardi, G.; Chanussot, J. Noise reduction in hyperspectral imagery: Overview and application. *Remote Sens.* **2018**, *10*, 482. [[CrossRef](#)]
- Xue, Y.J.; Wang, H.W.; Tian, Y.B.; Wang, Y.N.; Wang, Y.X.; Wang, S.M. Quantum information protection scheme based on reinforcement learning for periodic surface codes. *Quantum Eng.* **2022**, *2022*, 7643871. [[CrossRef](#)]
- Wang, H.; Song, Z.; Wang, Y.; Tian, Y.; Ma, H. Target-generating quantum error correction coding scheme based on generative confrontation network. *Quantum Inf. Process.* **2022**, *21*, 280. [[CrossRef](#)]

22. Wang, H.W.; Xue, Y.J.; Ma, Y.L.; Hua, N.; Ma, H.Y. Determination of quantum toric error correction code threshold using convolutional neural network decoders. *Chin. Phys. B* **2021**, *31*, 010303. [[CrossRef](#)]
23. Cao, Q.; Wang, H.W.; Qu, Y.J.; Xue, Y.J.; Wang, S.M. Quantum Teleportation Error Suppression Algorithm Based on Convolutional Neural Networks and Quantum Topological Semion Codes. *Quantum Eng.* **2022**, *2022*, 6245336. [[CrossRef](#)]
24. Zhang, X.M.; Kong, W.; Farooq, M.U.; Yung, M.H.; Guo, G.; Wang, X. Generic detection-based error mitigation using quantum autoencoders. *Phys. Rev. A* **2021**, *103*, L040403. [[CrossRef](#)]
25. Cerezo, M.; Arrasmith, A.; Babbush, R.; Benjamin, S.C.; Endo, S.; Fujii, K.; McClean, J.R.; Mitarai, K.; Yuan, X.; Cincio, L.; et al. Variational quantum algorithms. *Nat. Rev. Phys.* **2021**, *3*, 625–644. [[CrossRef](#)]
26. Haghshenas, R.; Gray, J.; Potter, A.C.; Chan, G.K.L. Variational power of quantum circuit tensor networks. *Phys. Rev. X* **2022**, *12*, 011047. [[CrossRef](#)]
27. Griol-Barres, I.; Milla, S.; Cebrián, A.; Mansoori, Y.; Millet, J. Variational quantum circuits for machine learning. an application for the detection of weak signals. *Appl. Sci.* **2021**, *11*, 6427. [[CrossRef](#)]
28. Macaluso, A.; Clissa, L.; Lodi, S.; Sartori, C. A variational algorithm for quantum neural networks. *Comput. Sci.* **2020**, *20*, 591–604.
29. Maheshwari, D.; Sierra-Sosa, D.; Garcia-Zapirain, B. Variational quantum classifier for binary classification: Real vs. synthetic dataset. *IEEE Access* **2021**, *10*, 3705–3715. [[CrossRef](#)]
30. Das, M.; Bolisetti, T. Variational Quantum Neural Networks (VQNNS) in Image Classification. *arXiv* **2023**, arXiv:2303.05860.
31. Huang, R.; Tan, X.; Xu, Q. Quantum Variational quantum tensor networks classifiers. *Neurocomputing* **2021**, *452*, 89–98. [[CrossRef](#)]
32. Ban, Y.; Torrontegui, E.; Casanova, J. Quantum neural networks with multi-qubit potentials. *Neurocomputing* **2023**, *13*, 9096. [[CrossRef](#)]
33. Higham, C.F.; Bedford, A. Quantum deep learning by sampling neural nets with a quantum annealer. *Sci. Rep.* **2023**, *13*, 3939. [[CrossRef](#)]
34. Chen, S.Y.-C. Efficient quantum recurrent reinforcement learning via quantum reservoir computing. *arXiv* **2023**, arXiv:2309.07339.
35. Alam, M.; Kundu, S.; Topaloglu, R.O.; Ghosh, S. Quantum-classical hybrid machine learning for image classification. *arXiv* **2021**, arXiv:2109.02862.
36. Naranjo-Torres, J.; Mora, M.; Hernández-García, R.; Barrientos, R.J.; Fredes, C.; Valenzuela, A. A review of convolutional neural network applied to fruit image processing. *Appl. Sci.* **2020**, *10*, 3443. [[CrossRef](#)]
37. Matsui, N.; Takai, M.; Nishimura, H. A network model based on qubitlike neuron corresponding to quantum circuit. *Phys. Electron. Commun. Jpn.* **2000**, *83*, 67–73. [[CrossRef](#)]
38. Maeda, M.; Suenaga, M.; Miyajima, H. A learning model in qubit neuron according to quantum circuit. *Adv. Nat. Comput.* **2005**, *1*, 283–292.
39. Masci, J.; Meier, U.; Cireşan, D.; Schmidhuber, J. Stacked convolutional auto-encoders for hierarchical feature extraction. *Int. Conf. Artif. Neural Netw.* **2011**, *21*, 52–59.
40. Lisnichenko, M.; Protasov, S. Quantum image representation: A review. *Quantum Mach. Intell.* **2023**, *5*, 2. [[CrossRef](#)]
41. Wu, J.; Tao, Z.; Li, Q. wpScalable Quantum Neural Networks for Classification. *arXiv* **2022**, arXiv:2208.07719.
42. Ren, W.; Li, W.; Xu, S.; Wang, K.; Jiang, W.; Jin, F.; Zhu, X.; Chen, J.; Song, Z.; Zhang, Z.; et al. Experimental quantum adversarial learning with programmable superconducting qubits. *Nat. Comput. Sci.* **2022**, *2*, 711–717. [[CrossRef](#)]
43. Paszke, A.; Gross, S.; Massa, F.; Lerer, A.; Bradbury, J.; Chanan, G.; Killeen, T.; Lin, Z.; Gimeshein, N.; Antiga, L.; et al. Pytorch: An imperative style, high-performance deep learning library. *Adv. Neural Inf. Process. Syst.* **2019**, *32*.
44. LeCun, Y.; Cortes, C.; Burges, C.J.C. MNIST Handwritten Digit Database. Available online: <http://yann.lecun.com/exdb/mnist/> (accessed on 4 February 2024).
45. Xiao, H.; Rasul, K.; Vollgraf, R. Fashion-MNIST: A Novel Image Dataset for Benchmarking Machine Learning Algorithms. Available online: <https://github.com/zalando-research/fashion-mnist> (accessed on 4 February 2024).
46. Suzuki, Y.; Kawase, Y.; Masumura, Y.; Hiraga, Y.; Nakadai, M.; Chen, J.; Nakanishi, K.M.; Mitarai, K.; Imai, R.; Tamiya, S.; et al. Qulacs: A fast and versatile quantum circuit simulator for research purpose. *Quantum* **2021**, *5*, 559. [[CrossRef](#)]
47. Konar, D.; Gelenbe, E.; Bhandary, S.; Sarma, A.D.; Cangi, A. Random quantum neural networks (RQNN) for noisy image recognition. *arXiv* **2022**, arXiv:2203.01764.
48. Konar, D.; Sarma, A.D.; Bhandary, S.; Bhattacharyya, S.; Cangi, A.; Aggarwal, V. A shallow hybrid classical–quantum spiking feedforward neural network for noise-robust image classification. *Appl. Soft Comput.* **2023**, *136*, 110099. [[CrossRef](#)]
49. Oh, S.; Choi, J.; Kim, J. A tutorial on quantum convolutional neural networks (QCNN). *arXiv* **2020**, arXiv:2009.09423.

Disclaimer/Publisher’s Note: The statements, opinions and data contained in all publications are solely those of the individual author(s) and contributor(s) and not of MDPI and/or the editor(s). MDPI and/or the editor(s) disclaim responsibility for any injury to people or property resulting from any ideas, methods, instructions or products referred to in the content.